Andrographolide suppresses epithelial mesenchymal transition by inhibition of MAPK signalling pathway in lens epithelial cells

FORUM KAYASTHA[1], KAID JOHAR[1], DEVARSHI GAJJAR[2], ANSHUL ARORA[1], HARDIK MADHU[1], DARSHINI GANATRA[1] and ABHAY VASAVADA[1,*]

[1]*Iladevi Cataract and IOL Research Centre, Gurukul road, Memnagar, Ahmedabad 380 052, India*

[2]*Department of Microbiology and Biotechnology Centre, Faculty of Science, MS University of Baroda, Vadodara 390 002, India*

**Corresponding author (Fax, 91-79-27411200; Email, icirc@abhayvasavada.com)*

Epithelial mesenchymal transition (EMT) of lens epithelial cells (LECs) may contribute to the development of posterior capsular opacification (PCO), which leads to visual impairment. Andrographolide has been shown to have therapeutic potential against various cancers. However, its effect on human LECs is still unknown. The purpose of this study is to evaluate the effect of andrographolide on EMT induced by growth factors in the fetal human lens epithelial cell line (FHL 124). Initially the LECs were treated with growth factors (TGF-β2 and bFGF) to induce EMT. Subsequently these EMT-induced cells were treated with andrographolide at 100 and 500 nM concentrations for 24 h. Our results showed that FHL 124 cells treated with growth factors had a significant decrease in protein and m-RNA levels of epithelial markers pax6 and E-Cadherin. After administering andrographolide, these levels significantly increased. It was noticed that EMT markers α-SMA, fibronectin and collagen IV significantly decreased after treatment with andrographolide when compared to the other group. Treatment with andrographolide significantly inhibited phosphorylation of ERK and JNK. Cell cycle analysis showed that andrographolide did not arrest cells at G0/G1 or G2/M at tested concentrations. Our findings suggest that andrographolide helps sustain epithelial characteristics by modulating EMT markers and inhibiting the mitogen-activated protein kinase (MAPK) signalling pathway in LECs. Hence it can prove to be useful in curbing EMT-mediated PCO.

[Kayastha F, Johar K, Gajjar D, Arora A, Madhu H, Ganatra D and Vasavada A 2015 Andrographolide suppresses epithelial mesenchymal transition by inhibition of MAPK signalling pathway in lens epithelial cells. *J. Biosci.* **40** 313–324] **DOI** 10.1007/s12038-015-9513-9

1. Introduction

Cataract is clouding or opacification of the lens. It is responsible for 51% of blindness in the world (WHO 2010). Posterior capsular opacification (PCO), also referred to as secondary cataract, is the most common postoperative complication of cataract surgery. PCO develops due to the presence of residual lens epithelial cells (LECs) after cataract surgery. A majority of these LECs undergo a process called epithelial mesenchymal transition (EMT) (Nathu *et al.* 2009). EMT is an orchestrated series of events in which interactions between cells as well as interactions between cells and the extracellular matrix (ECM) are altered to release epithelial cells from the surrounding tissue. The cytoskeleton is reorganized to confer the ability to move through a three-dimensional ECM, and a new transcriptional program is induced to maintain the mesenchymal phenotype (Radisky and LaBarge 2008). EMT of LECs results in the formation of fibroblasts and spindle-like myofibroblasts, which migrate to the posterior capsule resulting in vision impairment (Awasthi and Wagner 2006).

The transforming growth factor, beta 2 (TGF-β2), is known to induce EMT and inhibit proliferation of LECs (Hales *et al.* 1995). It has been shown that the basic fibroblast growth factor (bFGF) is involved in the development of PCO through aberrant LEC proliferation and differentiation (Cerra *et al.* 2003). PCO-like changes have been shown in rat explants by addition of a combination of TGF-β2 and

Keywords. Andrographolide; bFGF; epithelial mesenchymal transition; lens epithelial cells; MAPK signalling; TGF-β

Published online: 27 April 2015

bFGF (Symonds *et al.* 2006). Growth factors such as TGF-β2 and bFGF mediate cellular signalling through high-affinity cell surface receptors. The binding of these growth factors leads to activation of tyrosine kinase receptors and further downstream activation of distinct pathways such as the mitogen-activated protein kinase (MAPK) pathway (Lin *et al.* 1998). The MAPK pathway has been implicated in the development of PCO (Dawes *et al.* 2009). EMT can be induced in LECs under the influence of TGF-β2 and bFGF (Symonds *et al.* 2006). Hence LECs provide a model to evaluate the effect of various drugs in preventing EMT.

Andrographolide is a labdane diterpenoid, the main bioactive component of the medicinal plant *Andrographis paniculata*. Andrographolide is known to have pharmacological effects such as anti-fibrotic, anti-inflammatory, and anti-cancerous effects (Rana and Avadhoot 1991, Akbarsha and Murugaian 2000, Shen *et al.* 2000, Li *et al.* 2007, Shen *et al.* 2009, Lee *et al.* 2010a). Andrographolide is known to interfere, either directly or indirectly, with several major signalling pathways (Tsai *et al.* 2004, Ji *et al.* 2007, Lee *et al.* 2010b, Cheung *et al.* 2012).

Postsurgical prevention of LEC proliferation, migration, and EMT would be a possible option to prevent PCO. Several drugs (Biswas *et al.* 1999, Rabsilber and Auffarth 2006, Chandler *et al.* 2007) have been tried to prevent PCO but none of them have shown promising results. Further, a majority of the drugs cause damage to the surrounding tissues. Therefore, it is necessary to find a drug or compound, which has a low level of toxicity and is effective in controlling growth factor-induced EMT for the prevention of PCO.

From the current information, it is evident that there is a need to explore the potential andrographolide has in preventing EMT in LECs. In this study, we speculated the anti-fibrotic property of andrographolide on the human lens epithelial cell line (FHL 124) treated with growth factors (TGF-beta and bFGF). In this growth factor-induced EMT model, we analysed the expression of epithelial and EMT markers. Further, we also analysed the role played by andrographolide in the MAPK signalling pathway and cell cycle events.

2. Materials and methods

The reagents TGF-β2 and bFGF were purchased from Invitrogen, Carlsbad, CA, USA. The MAPK inhibitor (PD98059) was purchased from Cell Signaling Technology, MA, USA. Antibodies such as pERK, total ERK, pJNK, and total JNK were purchased from BD Biosciences, Franklin Lakes, NJ, USA. Andrographolide was purchased from Sigma Aldrich, St. Louis, MO. Stock solutions of andrographolide were prepared in dimethyl sulfoxide (DMSO). These stock solutions were diluted in cell culture media to obtain a final concentration of 100nM and 500nM. A stock solution of PD98059 was prepared in DMSO and diluted in the media to obtain a final concentration of 20 μM. TGF-β2 was suspended in phosphate-buffered saline (PBS) containing 0.1% bovine serum albumin (BSA) to obtain a concentration of 10 μg/mL, which was further diluted in cell culture media to a final concentration of 10 ng/mL. The growth factor bFGF was suspended in PBS containing 0.1% BSA to obtain a concentration of 10 μg/mL which was diluted in cell culture media to 40 ng/mL.

2.1 *Cell culture and viability*

The fetal human lens epithelial cell line (FHL 124) (a kind gift from Dr John R Reddan, Oakland University, Michigan, USA) was grown in Eagle's Minimum Essential Media (Sigma, St. Louis, MO), containing 10% fetal bovine serum (Sigma, St. Louis, MO) and 50 μg/mL gentamycin at 35°C in a humidified 5% CO_2 atmosphere. For the viability assay, cells were seeded in 96-well plates (8×10^3 cells per well). Cells were treated with different concentrations of andrographolide, 0.1% DMSO (negative control) or staurosporin (positive control) for 24 h. Thereafter 20 μL of 3-(4,5-dimethylthiazol-2-yl)-2,5-diphenyltetrazolium bromide(MTT) solution (5 mg/mL in PBS) was added and the cells were incubated for 4 h at 35°C. The purple formazan crystals were dissolved in 150 μL of DMSO. The plates were read at 570 nm. The absorbance values were expressed as a percentage over the control group in which no treatment was administered.

2.2 *Cell culture and treatments*

For treatments 70% confluent cells were made serum-free. The cells were divided into six treatment groups. The cells were treated with growth factors [TGF-β2 (10 ng/mL), bFGF (40 ng/mL)] abbreviated as GFs and andrographolide (100 or 500nM), either alone or in a combination for 24 h. The following abbreviations were used for the various treatments groups: Normal (no treatment), Control [TGF-β (10 ng/mL) + bFGF (40 ng/mL)], GFs + A100 [GFs + Andro (100 nM)], GFs + A500 [GFs + Andro (500 nM)], A100 [Andro (100 nM)], and A500 [Andro (500 nM)]. In order to evaluate the effect of MAPK signalling, some cultures were also exposed to the MAPK Inhibitor (PD 98059) (20 μM), 1 h prior to addition of growth factors as per the manufacturer's protocol. The final concentration of DMSO in the medium was not more than 0.1% (v/v). At this concentration, DMSO had no effect on cell growth. After treatment, cells were harvested for immunofluorescence, protein, and m-RNA analysis. All experiments were performed in triplicates or otherwise mentioned.

2.3 *Immunofluorescence*

FHL 124 cells were grown on a gelatin coated cover-slip in a 12-well culture plate. Cells were fixed in 2% paraformaldehyde for 15 min and permeabilized with 0.25% Triton-X in

PBS for 10 minutes. Subsequently cells were incubated with primary antibodies (1:100), pax6 (Abcam, Cambridge, UK), α-SMA (Sigma, St. Louis, MO, USA), collagen IV (Sigma), vimentin (Sigma) for 1 h. After 3 rinses of PBS containing 0.05% Tween-20 (PBST) for 3 minutes each, the cells were incubated with fluorescent-tagged secondary antibodies (Alexa fluor 546 Goat Anti-Rabbit and Alexa fluor 488 Goat Anti-Mouse obtained from Invitrogen). An epifluorescence microscope (Axioskope II; Carl Zeiss, Oberkochen, Germany) was used to observe the cells and images were documented with a CCD camera (Cohu, San Diego, CA, USA). Corrected total cell fluorescence (CTCF) for pax6 was calculated by formula, CTCF = Integrated Density − (Area of selected cell × Mean fluorescence of background readings) by using Image J software.

2.4 *Western blotting*

FHL 124 cells were grown in 25 cm^2 flasks and treated at approximately 70% confluence as mentioned earlier. Cells were washed in PBS and lysed in buffer (50 mM Tris pH 7.4, 150 mM NaCl, 1% Triton-X 100, 0.1% SDS, 0.5% sodium deoxycholate) supplemented with protease inhibitor cocktail and phosphatase inhibitor cocktail tablets (Roche Diagnostics, Grenzacherstrasse 124, Basel, Switzerland). The protein concentrations were quantified using a bicinchoninic acid assay. The samples containing 20 μg protein were separated on 8% or 10% SDS-PAGE and then electrophoretically transferred to nitrocellulose membranes (Pall Corporation, Port Washington, NY, USA). The membranes were blocked at room temperature for 1 h in tris-buffered saline with Tween®20 (TBST) (10 mM Tris-HCl [pH 7.6], 150 mM NaCl, 0.05% Tween-20) containing 5% non-fat dry milk and incubated overnight with anti-pax6, fibronectin, α-SMA, E-Cadherin, collagen IV, vimentin, b-actin, ERK, pERK (pT202/pY204), JNK and pJNK (pT183/pY185) antibodies at 1: 1000 dilution at 4°C. The membranes were washed with TBST and incubated with horseradish peroxidase (HRP) conjugated secondary antibodies (CST) at 1:2000 dilution. After washing with TBST, the bands were developed by the chemiluminescence technique using Luminata Forte (Millipore). Blots were stripped using a mild buffer (0.2 M glycine, 0.1% SDS, 1% Tween 20, pH 2.2), washed with PBS and TBST, and blocked with 5% non-fat dry milk in TBST. The blots were then re-probed with different antibodies and developed again using the same method. The densitometry analysis for relative band intensity was done using Image J software (NIH Image).

2.5 *Quantitative PCR*

Cells were washed with PBS and collected in a TRIZOL reagent (Invitrogen, Carlsbad, CA, USA). RNA was extracted according to the manufacturer's instructions. Four μg of total RNA was reverse transcribed at 25°C for 5 min, at 42°C for 60 min, and at 70°C for 5 min in 20 μL of 1 μg of oligo (dT), 1 μg of random hexamer, 20 pmol primer, 3 mM MgCl2, 0.05 mM of dNTPs, 4 μL of Genei™ 5×reaction buffer, 1 unit of Recombinant RNasin® Ribonuclease Inhibitor, and 1 μL of Genei™ Reverse Transcriptase (All chemicals from GeneI Bangalore, Karnataka, India). For quantitative PCR, amplifications were performed on the LightCycler®480 (Roche) in 20 μL of reaction using 2 μL of cDNA, 10 μL of SYBR Green I Master (Roche), and gene-specific primers of 2.5 μM concentration. The amplification was carried out at 95°C for 10 min before the first cycle, 95°C for 15 seconds, and 60°C for 60 s repeated 40 times. Quantitative PCR was performed for *PAX6*, *ACTA2*, *CDH1*, *COL4A1*, *FN1*, and *VIM* and *ACTB* was used as housekeeping gene. The sequence of primers was obtained from qPrimerDepot online software (Table 1). Relative expression, normalized to the housekeeping gene, was calculated using LightCycler®480 Software (Roche).

2.6 *Cell cycle analysis*

After treatment, cells were trypsinized, centrifuged, and fixed in 70% ethanol for 1 h at 4 °C. After washing with PBS, cells were stained overnight with 25 μg/mL of propidium iodide. 10 μg/mL of RNase A, 0.2% of Saponin, and 0.1mM of EDTA at 4°C. The stained cells were then filtered through a 40 μm pore-sized nylon mesh to ensure single cell suspension. The cells were subsequently subjected to analysis using the flow cytometer (FACS ARIA Becton Dickinson, Franklin Lakes, NJ, USA). In each sample, ten thousand cells were analysed and the cell cycle distribution was calculated using FACSDiva software (version 6.1.3) (Becton Dickinson).

Statistical Analysis: Statistical significance was determined by a two-tailed student's t-test and a difference of $p<0.05$ was considered statistically significant.

3. Results

3.1 *IC 50 value of andrographolide*

To determine the IC 50 value of andrographolide on cell viability, FHL 124 cells were treated with 0.1 -1000 μM of andrographolide for 24 h. Cell viability was assessed using the MTT assay. The percentage of cell viability was calculated by considering the controls as 100%. Andrographolide treatment resulted in loss of cell viability in a dose-dependent manner. The dose-response curve (figure 1) shows that IC 50 was 1μM.

Table 1. List of primers used in the study

No.	Gene name	Forward primer	Reverse Primer	Tm
1.	ACTB	GTTGTCGACGACGAGCG	GCACAGAGCCTCGCCTT	56.4/58.3
2.	PAX6	TCCGTTGGAACTGATGGAGT	GTTGGTATCCGGGGACTTC	56.0/55.1
3.	ACTA2	CCAGAGCCATTGTCACACAC	CAGCCAAGCACTGTCAGG	56.3/56.4
4.	CDH1	CTTGCGGAAGTCAGTTCAGA	CAGAGCCAAGAGGAGACCTG	54.8/57.1
5.	COL4A1	CCTTTTGTCCCTTCACTCCA	CTCCACGAGGAGCACAGC	60.4/64.5
6.	FN1	GGTGGAATAGAGCTCCCAGG	GCAGCCTGCATCTGAGTACA	64.5/62.4
7.	VIM	ATTCCACTTTGCGTTCAAGG	CTTCAGAGAGAGGAAGCCGA	53.7/55.9

3.2 *Cell morphology*

Morphological changes were noticed in FHL 124 cells after subjecting them to 24 h of growth factor treatment. The cells were elongated and attained a spindle-shaped morphology similar to EMT changes. The morphological changes were suppressed by co-treatment of andrographolide at 500 nM concentration (figure 2A).

3.3 *Effect of andrographolide on expression of pax6 and E-Cadherin*

Treatment of FHL 124 cells with growth factors for 24 h resulted in a significant down-regulation of m-RNA by 8.15 ($p<0.05$) fold and protein level of Pax6 by 1.50 ($p<0.05$) fold. There was down-regulation of E-Cadherin in m-RNA level by 10.13 fold ($p<0.05$) and protein level by 10.28-fold ($p<0.02$) in the control group when compared to the normal group (figure 3A, B, D and E). In concurrence with this, immuno-fluorescence staining of pax6 was also weakened (figure 3F).

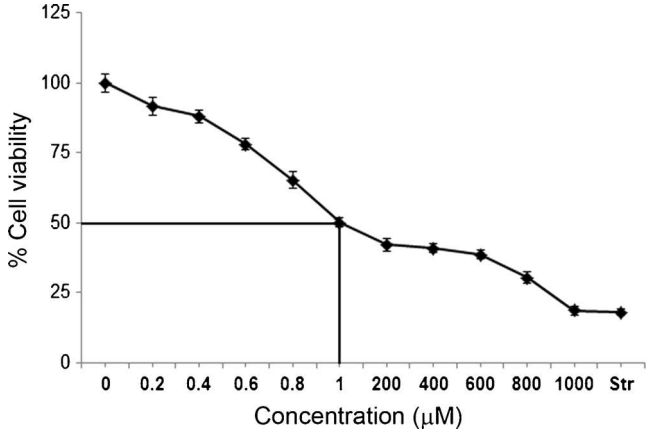

Figure 1. To evaluate the effect of andrographolide on cell viability. FHL 124 cells were treated with 0.1–1000 μM of andrographolide for 24 h. Andrographolide treatment resulted in loss of cell viability in a dose-dependent manner. The dose response curve shows IC 50 was 1μM.

On the contrary, treatment with andrographolide resulted in significant up-regulation of m-RNA and protein levels of pax6 and E-Cadherin (figure 3A, B, D and E) as well as a retrieval of the staining of pax6 in FHL 124 cells (figure 3F). CTCF of pax 6 corroborates with staining pattern (figure 3G). Expression of pax6 and E-Cadherin does not change significantly in A100 and A500 groups when compared to the normal groups.

3.4 *Effect of andrographolide on expression of α-SMA and fibronectin*

We wanted to explore whether andrographolide could prevent TGF-β2 and bFGF-induced EMT expression of α-SMA and fibronectin. As shown in figure 4, GFs increased the expression at m-RNA and protein levels of α-SMA by 6.05 ($p<0.05$) and 1.79 ($p<0.05$) folds and fibronectin by 1.76 ($p<0.05$) and 3.02 ($p<0.05$) folds when compared to the normal group. In agreement with these findings, immuno-fluorescent staining of α-SMA and fibronectin was enhanced. α-SMA was expressed in the form of elongated stress fibres in the cytoplasm and fibronectin was localized as a dense network of fibres in ECM. Treatment with andrographolide completely abrogated up-regulation of α-SMA and fibronectin (figure 4 A, B, D and E) as well as weakened their staining in FHL 124 cells (figure 4F). Expression of α-SMA was down-regulated by 7.89 (**$p<0.02$) fold in the A500 group when compared to the normal.

3.5 *Effect of andrographolide on the expression of vimentin and collagen IV*

Expression of vimentin and collagen IV also increases during EMT. Treatment with TGF-β2 and bFGF resulted in 1.88 ($p<0.05$) fold up-regulation of m-RNA and 2.08 ($p<0.02$) fold up-regulation of protein expression of vimentin while collagen-IV increased by 6.11 ($p<0.05$) and 3.28 ($p<0.05$) folds in the control group as compared to the normal group. Immuno-fluorescent staining showed that collagen IV was localized as a dense network of fibres around the cells and its intensity increased in control group. Andrographolide treatment resulted in down-regulation of collagen IV at m-RNA and protein levels

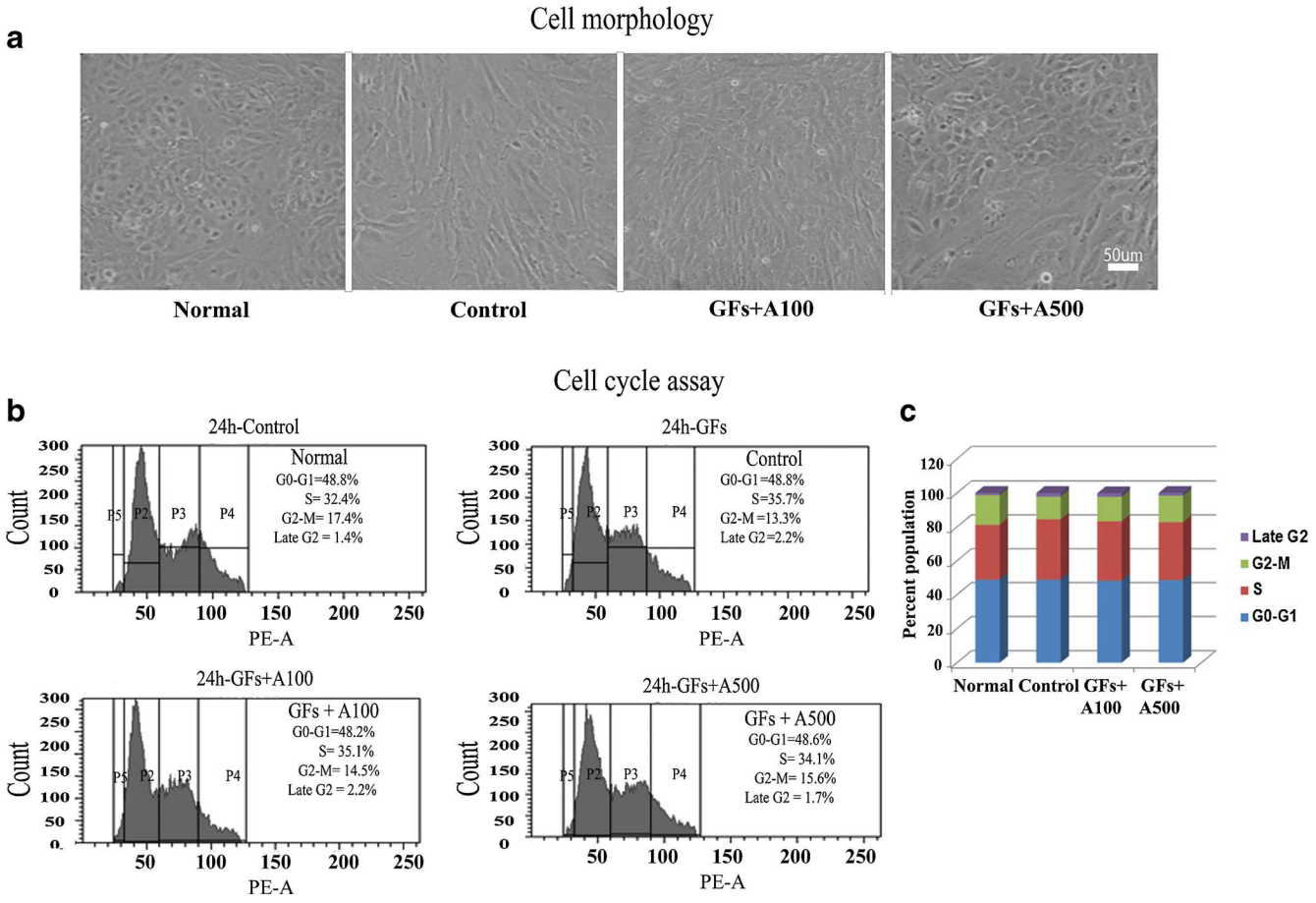

Figure 2. (**a**) Inhibitory effect of andrographolide on TFG-β2 and bFGF-induced fibroblastic phenotype in FHL 124 cells. There was no change in morphology in FHL 124 cells after 24 h of treatment with 500nM andrographolide compared with the normal cells. Treatment with TFG-β2 and bFGF resulted in elongation and spindle-like morphology in FHL 124 cells, which was suppressed by co-treatment of andrographolide. (**b**) Cell count in different phases of the cell cycle; P1 – total number of cells, cells in P2 – G0-G1, P3 – S, P4 – G2-M and P5 – late G2 in groups. Cell cycle analysis showed percent population (**c**) of cells in phases of the cell cycle in different experimental groups (NS, non-significant).

(figure 5A, D). Immuno-fluorescent staining suggested that the intensity of collagen IV decreases and was almost absent in the GFs+A500 group. Andrographolide treatment does not bring about a significant change in expression of vimentin at protein and m-RNA levels. Vimentin was localized in the form of elongated fibres in the cytoplasm and their expression increased in the control group (figure 5F).

3.6 *Effect of andrographolide on the MAPK signalling pathway*

Our results show that treatment of growth factors in FHL 124 cells induced the MAPK signalling pathway. Growth factors significantly induced phosphorylation of ERK (pT202/pY204) by 1.48 ($p<0.05$) fold and JNK (pT183/pY185) by 1.68 ($p<0.02$) fold respectively. The results show that treatment of PD 98059 and andrographolide results in significant inhibition of phosphorylation of ERK by 1.60 ($p<0.05$) fold in the GFs+PD group, 2.06 ($p<0.02$) fold in the GFs+A100 group and 8.24 ($p<0.01$) fold in the GFs+A500 group (figure 6B). Further pJNK down-regulated by 1.92 ($p<0.01$) fold in GFs+PD group, by 5.74 ($p<0.01$) fold in the GFs+A100 group and 11.03 ($p<0.01$) fold in the GFs+A500 group (figure 6C). pERK expression was down-regulated by 5.60 ($p<0.01$) and 5.74 ($p<0.01$) folds and pJNK by 3.25 ($p<0.05$) and 3.29 ($p<0.01$) folds in A100 and A500 groups when compared to the normal.

3.7 *Effect of andrographolide on the cell cycle*

Andrographolide has been shown to induce cell cycle arrest at the G1 or G2/M phase in different cell types (Cheung *et al.*

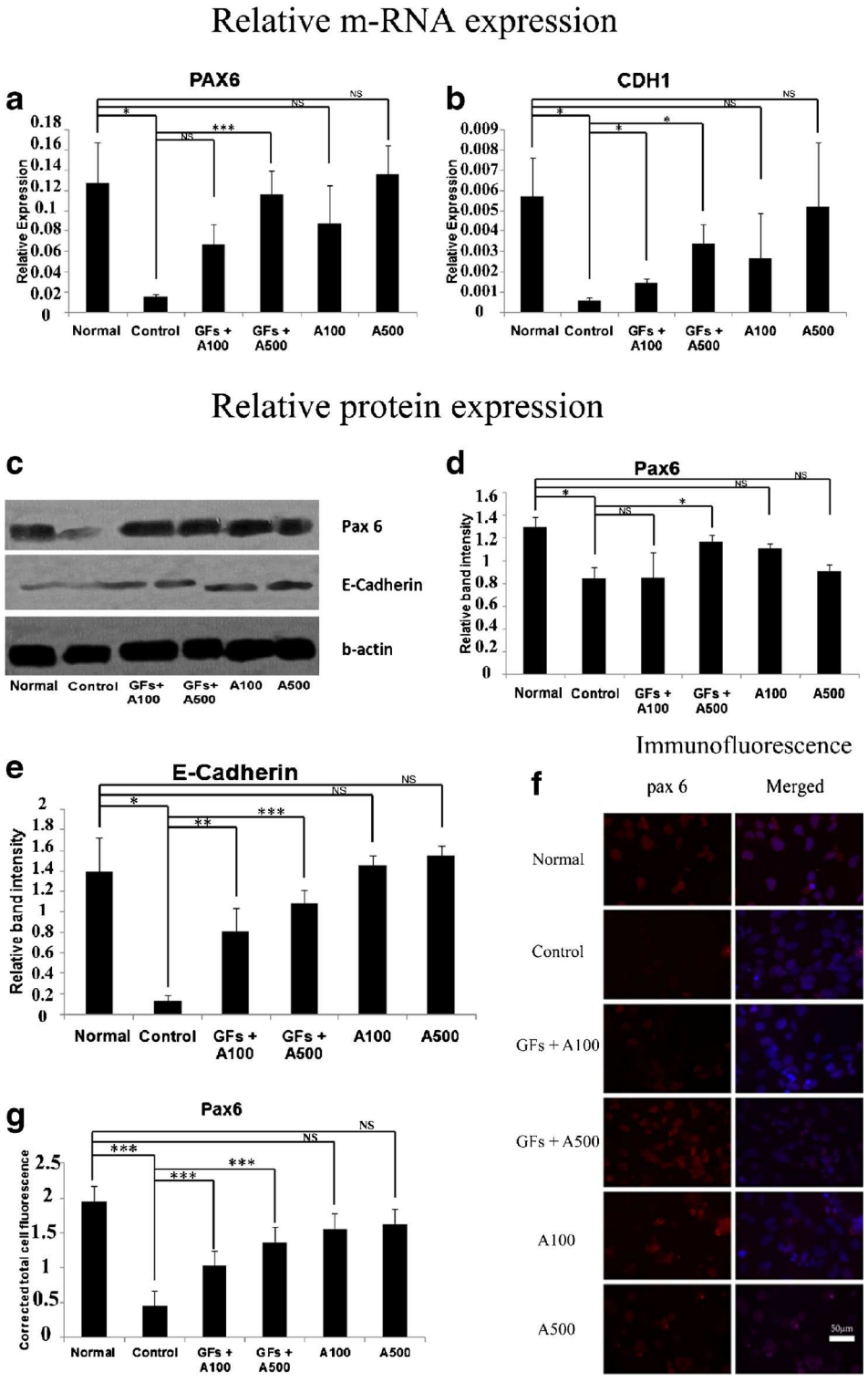

Figure 3. Exposure of TGF-β and bFGF results in loss of pax6 and E-Cadherin. Co-treatment of andrographolide regains levels of pax6 and E-Cadherin in FHL 124 cells. Andrographolide co-treatment with growth factors at concentrations of 100 and 500 nM results in up-regulation of (**a**) *PAX6* by 4.27 (NS) and 7.42 (**p<0.01) (n=5) and (**b**) *CDH1* by 2.57 (*p<0.05) and 5.97 (*p<0.05) (n=5), (**c**) Immunoblots of Pax6, E-Cadherin and b-actin, (**d**) Protein levels of pax6 by 1.00 (NS) and 1.37 (*p<0.05) and (**e**) E-Cadherin by 5.97 (*p<0.05) and 7.99 (***p<0.01) fold when compared to the control group. (**f**) Pax6 was localized in the nucleus (red). Nucleus was counterstained by DAPI (blue). (**g**) CTCF of pax 6 (***p<0.01).

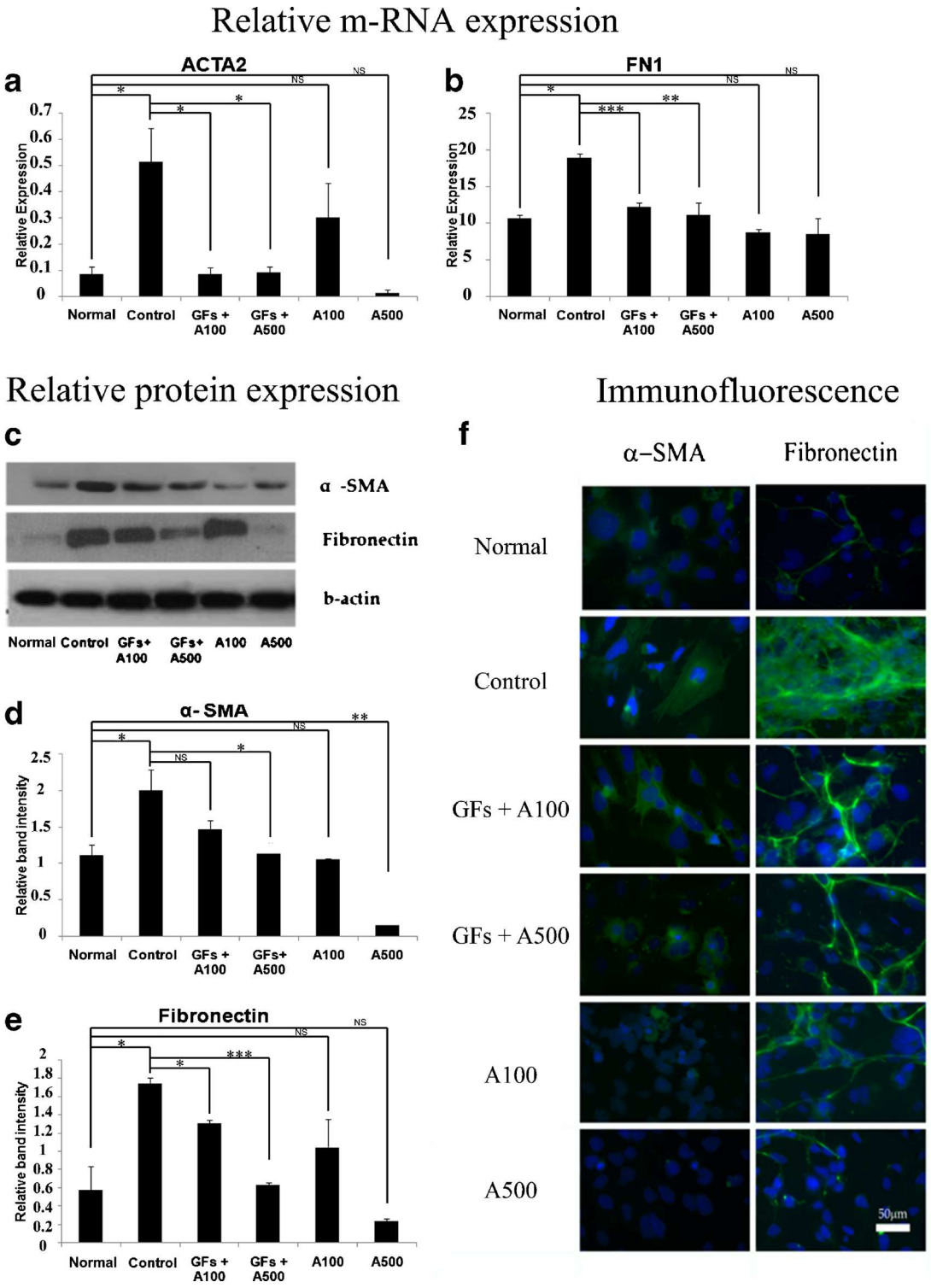

Figure 4. Exposure of TGF-β and bFGF increases expression of EMT markers, α-SMA and fibronectin. Co-treatment of andrographolide abrogates the expression of α-SMA and fibronectin in FHL 124 cells. Andrographolide co-treatment with growth factors at concentrations of 100 and 500nM results in down-regulation of (**a**) *ACTA2* by 6.01 (*p<0.05) and 5.72 (*p<0.05) (n=5) and (**b**) *FN1* by 1.55 (***p<0.01) and 1.70 (**p<0.02) folds (n=5), (**c**) Immunoblots of α-SMA, Fibronectin and b-actin, (**d**) α-SMA was down-regulated by 1.36 (NS) and 1.77 (*p<0.05) and (**e**) fibronectin by 1.30 (*p<0.05) and 2.77 (***p<0.01) folds when compared to the control group. (**f**) Immunofluorescent staining showed α-SMA in cytoplasm. Fibronectin was located outside the cell margin. The nucleus was counterstained with DAPI.

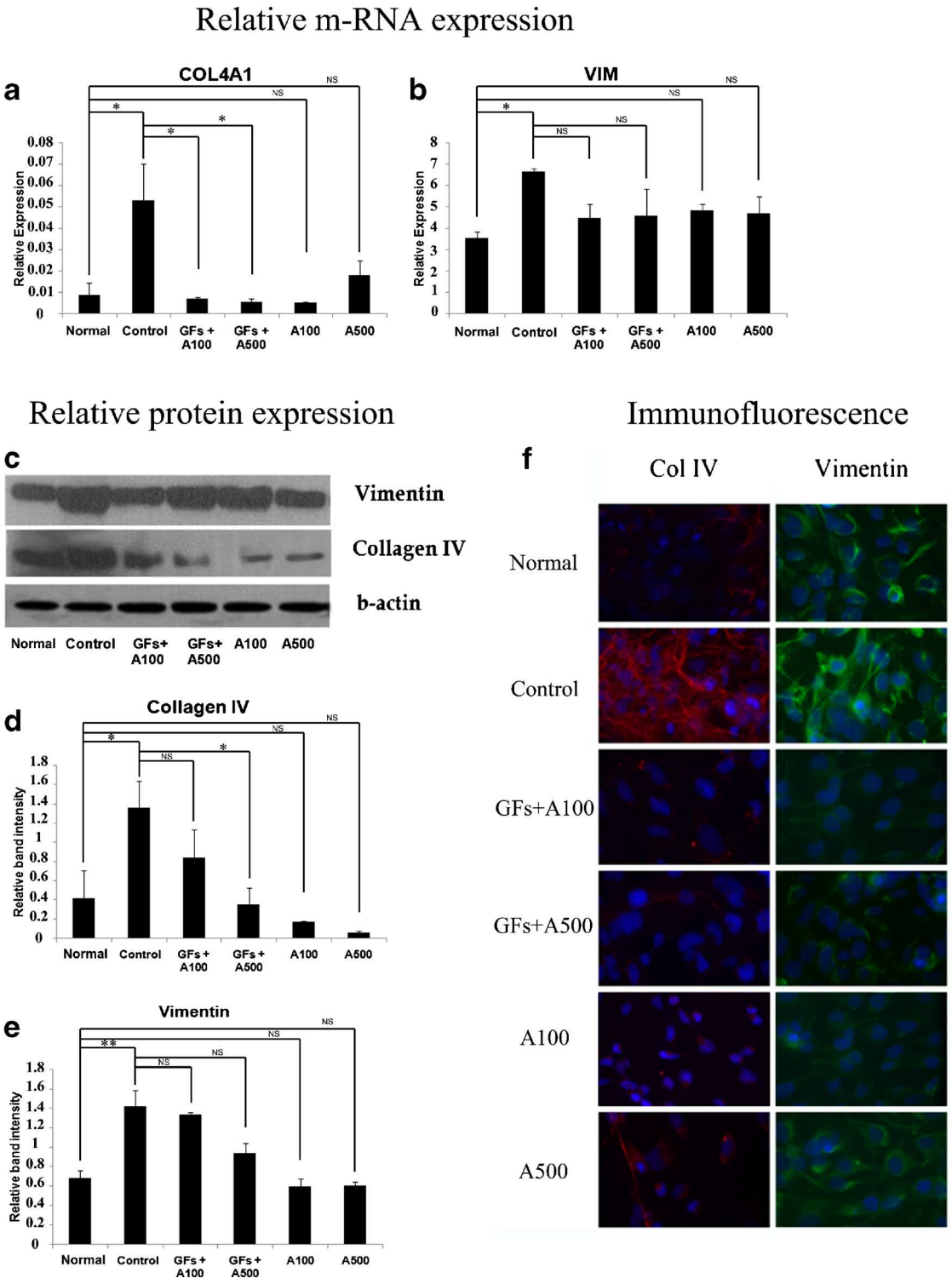

Figure 5. Exposure to TGF-β and bFGF increases expression of collagen IV and vimentin. Co-treatment with andrographolide decreases the expression of collagen IV and vimentin in FHL 124 cells. Andrographolide co-treatment with growth factors at concentrations of 100 and 500 nM results in (**a**) down-regulation of *COL4A1* by 7.68 (*p<0.05) and 10.02 (*p<0.05) (n=5), (**c**) Immunoblots of Vimentin, Collagen IV and b-actin, (**d**) collagen IV by 1.61 (NS) and 3.81 (*p<0.05) when compared to the control group. (**b**, **e**) However, expression of vimentin does not change significantly after andrographolide treatment when compared to the control group. (**f**) Vimentin was localized in the form of elongated stress fibres. Collagen IV was located outside the cell margin. The nucleus was counterstained with DAPI.

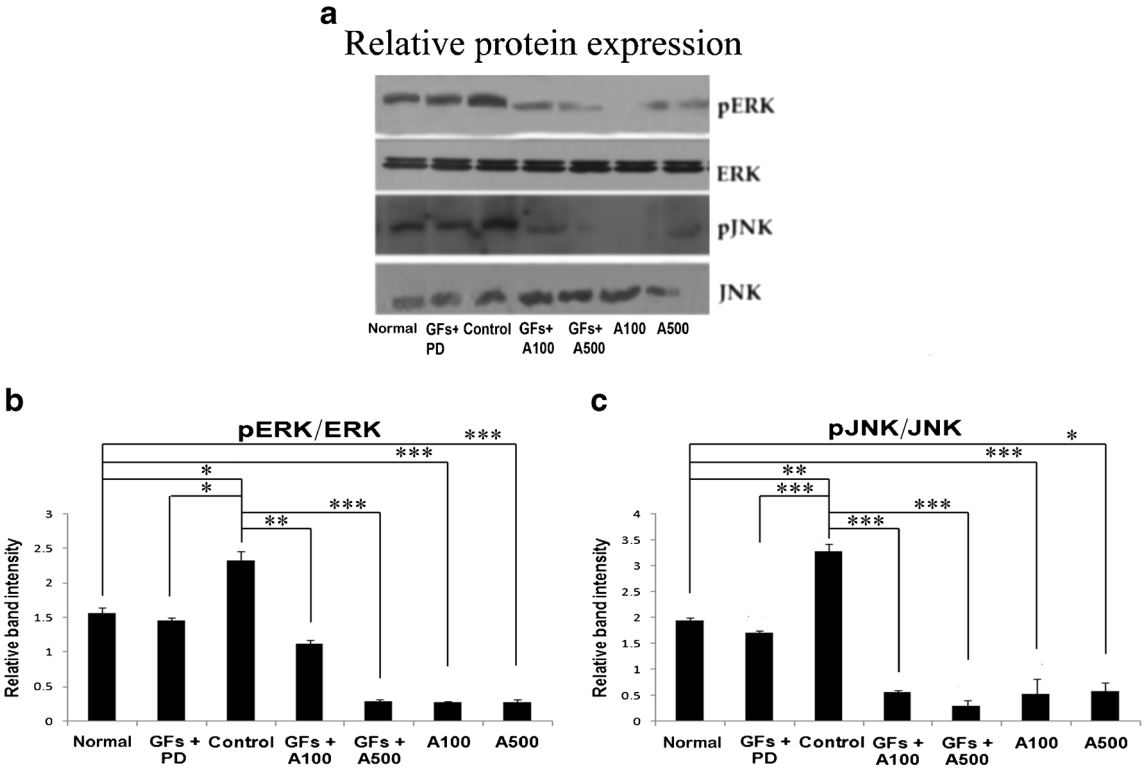

Figure 6. Exposure to TGF-β and bFGF increases expression of pERK and pJNK in FHL 124 cells. (**a**) Co-treatment with andrographolide decreases the expression of pERK and pJNK in FHL 124 cells. Relative protein expression of pERK and pJNK was given with reference to total ERK and JNK respectively (**b** and **c**) (*p<0.05, **p<0.02 and ***p<0.01).

2012). Cell cycle analysis showed the percent population of cells in different phases of the cell cycle in experimental groups (figure 2B). The percentage difference between the normal and treated groups for each phase were calculated and results showed that there was a mild increase in percentage of cells in the S phase. However, the changes were not significant in control, GFs+A100, and GFs+A500 when compared to the normal (figure 2C). Andrographolide does not arrest FHL 124 cells at 100 and 500 nM concentrations when treated for 24 h.

4. Discussion

To our knowledge, this is the first study to show the ameliorative effect of andrographolide on TGF-β2 and bFGF-induced EMT of LECs (FHL 124), the cells mainly involved in the development of PCO (a systematic electronic literature search from 1998 to early 2014 was undertaken using the online databases PubMed and Google Scholar). The effect of andrographolide seems to occur in a dose-dependent manner. There was no significant cytotoxic effect at the concentrations (100 and 500 nM) used in the study.

Many *in vitro* and *ex vivo* models of TGF-β2-induced anterior subcapsular cataract (ASC) and PCO have been developed (Liu *et al.* 1996, Wormstone *et al.* 1997, Wormstone *et al.* 2002, Wormstone *et al.* 2006). TGF-β2-induced EMT of LECs appears to play a key role in PCO. TGF-β2 is the major isoform within the eye, most of which is detected in the aqueous humor and exists largely in the latent form. However, after trauma (e.g., by surgical injury), active levels of all TGF-β isoforms can be elevated (Dawes *et al.* 2009). TGF-β2 is known to inhibit LEC proliferation and induce apoptosis (Mansfield *et al.* 2004). The growth factor bFGF is normally present in the lens environment and its concentration may increase after cataract surgery (Wormstone *et al.* 2001). Studies have shown that bFGF induces LEC proliferation, which may contribute to the development of PCO. The growth factor bFGF has been shown to exacerbate TGF-β2-induced anterior subcapsular cataract in cultured rat lenses (Cerra *et al.* 2003). On testing, it was observed that other growth factors did not have this effect. Other features of PCO such as excessive deposition of extracellular matrix (ECM) and formation of plaques of swollen cells occurred only when TGF-β2 was supplemented with bFGF (Apple *et al.* 1992) (Mansfield *et al.* 2004). This

suggests that addition of bFGF induces proliferation, which eventually counteracts the proliferation suppression of LECs by endogenous TGF-β2. The human lens cell line FHL 124 has been used in recent years to investigate the effects of TGF-β2-induced transdifferentiation and contraction (Dawes *et al.* 2007a, Eldred *et al.* 2011). Hence, in our study, we have used a combination of TGFβ-2 and bFGF to induce EMT in FHL 124 cells to mimic PCO-like conditions. We have previously reported that andrographolide reduces proliferation and migration of FHL 124 cells by inhibition of PI3K/Akt pathway (Kayastha *et al.* 2014).

Pax6 plays an important role in lens development and its expression is confined to the lens epithelium (Kerr *et al.* 2012). TGFβ signalling could lower pax6 expression in FHL 124 cells (Dawes *et al.* 2007b, Grocott *et al.* 2007). During EMT, LECs initially lose their cell-to-cell contact due to reduced expression of the cell adhesion molecule, E-Cadherin. This is followed by multi-layering of the cells and their subsequent transdifferentiation into myofibroblasts (Nathu *et al.* 2009). In our results, expression of m-RNA and protein levels of Pax6 and E-Cadherin decreased in the growth factor-induced group and these levels were regained following andrographolide treatment. Moreover, to facilitate mesenchymal phenotype transdifferentiation, markers like α-SMA, fibronectin, collagen IV and vimentin were up-regulated (Banh *et al.* 2006, Choi *et al.* 2007, Gotoh *et al.* 2007). During pathogenesis of PCO, lens cells aberrantly synthesize and deposit ECM components, which results in obscured vision. TGF-β2-induced fibrotic markers such as α-SMA, fibronectin and matrix contraction/wrinkling of the posterior capsule play a major role in PCO formation (Wormstone *et al.* 2002). In our results, m-RNA and protein expression of α-SMA, fibronectin, collagen IV and vimentin were significantly up-regulated in the growth-factor-induced group, while andrographolide treatment completely abrogated the up-regulation of α-SMA, fibronectin and collagen IV. Andrographolide is reported to arrest the cell cycle depending on the cell type and concentration (Cheung *et al.* 2012). However, our results show that andrographolide was unable to arrest FHL 124 cells at a given time and concentration.

Recent studies have also shown TGF-β2-mediated EMT through SMAD independent pathways like ras/MEK/ERK MAP kinase cascade, Rho Kinase, JNK and p38MAPK. MAPK signalling was found to play a role in matrix contraction, a phenomena occurring during PCO (Dawes *et al.* 2009). Exposure of TGF-β2 leads to serine/threonine phosphorylation. Moreover TGF-beta RII undergoes autophosphorylation on tyrosine residues (Lawler *et al.* 1997). Further studies from Galliher and Schiemann showed that Src-mediated tyrosine phosphorylation of TGF-beta RII triggers receptor in activation of the MAPK pathway (Nakerakanti and Trojanowska 2012). Moreover, the presence of bFGF can activate the ERK pathway that has been shown to play a role in fibre differentiation (Wang *et al.* 2009). In our study, exposure of FHL 124 cells to growth factors led to activation of the MAPK pathway. We have used PD98059, which is an inhibitor of ERK1 and ERK2. Moreover PD98059 has been reported to block phosphorylation of JNK (Salh *et al.* 2000). In accordance with previous reports, PD98059 suppressed phosphorylation of ERK and JNK induced by exposure to growth factors. Treatment of FHL 124 cells with andrographolide results in suppression of phosphorylation of ERK and JNK at protein levels.

Andrographolide is known for various biological activities such as anti-tumoral (Rajagopal *et al.* 2003), antibacterial, anti-inflammatory and immunostimulant activities (Kumar *et al.* 2004). Andrographolide has been reported to be antifibrotic as it reduces TGF-β and α-SMA expression in hepatic cells (Lee *et al.* 2010a). We hypothesize that andrographolide suppressed EMT-mediated effects by inhibiting the MAPK signalling pathway. Andrographolide treatment is known to activate macrophages and reduce the level of ERK 1/2 phosphorylation (Wang *et al.* 2010). Andrographolide has been shown to inhibit v-Src-induced transformation in the cancer cell line. Oncogenic Src proteins in epithelial cells have been reported to induce EMT. Src kinases perturb multiple intracellular signalling pathways. One of them is the MAPK pathway, which has been shown to be essential for v-Src-induced neoplastic transformation (Liang *et al.* 2008). The role of Src kinases has been well identified in the induction of PCO (Walker *et al.* 2007). It is reported that andrographolide significantly reduces the expression level of v-Src protein in a concentration-dependent manner. We hypothesize that the inhibition of MAPK signalling may be the result of direct interference with ERK and JNK signalling or down-regulation of Src kinases. The effect of andrographolide on the SMAD signalling pathway in EMT-induced LECs could provide crucial information regarding the role of andrographolide in EMT.

Andrographolide helps to sustain epithelial characteristics by modulating EMT markers and inhibiting the MAPK signalling pathway in lens epithelial cells. Hence, it could be useful in curbing EMT-mediated PCO.

Acknowledgements

FK is a recipient of the INSPIRE Fellowship (IF110617) and is thankful to the Department of Science and Technology (DST) for the same. The authors thank Mr Dhanir Tailor for his technical help.

References

Akbarsha MA and Murugaian P 2000 Aspects of the male reproductive toxicity/male antifertility property of andrographolide in albino rats: effect on the testis and the cauda epididymidal spermatozoa. *Phytother. Res.* **14** 432–435

Apple DJ, Solomon KD, Tetz MR, Assia EI, Holland EY, Legler UF, Tsai JC, Castaneda VE, *et al*. 1992 Posterior capsule opacification. *Surv. Ophthalmol.* **37** 73–116

Awasthi N and Wagner BJ 2006 Suppression of human lens epithelial cell proliferation by proteasome inhibition, a potential defense against posterior capsular opacification. *Invest. Opthalmol. Vis. Sci.* **47** 4482–4489

Banh A, Bantseev V, Choh V, Moran KL and Sivak JG 2006 The lens of the eye as a focusing device and its response to stress. *Prog. Retin. Eye. Res.* **25** 189–206

Biswas NR, Mongre PK, Das GK, Sen S, Angra SK and Vajpayee RB 1999 Animal study on the effects of catalin on aftercataract and posterior capsule opacification. *Ophthalmic. Res.* **31** 140–142

Cerra A, Mansfield KJ and Chamberlain CG 2003 Exacerbation of TGF-beta-induced cataract by FGF-2 in cultured rat lenses. *Mol. Vis.* **9** 689–700

Chandler HL, Barden CA, Lu P, Kusewitt DF and Colitz CM 2007 Prevention of posterior capsular opacification through cyclooxygenase-2 inhibition. *Mol. Vis.* **13** 677–691

Cheung MT, Ramalingam R, Lau KK, Chiang WL and Chiu SK 2012 Cell type-dependent effects of andrographolide on human cancer cell lines. *Life Sci.* **91** 751–760

Choi MS, Yoo MS, Son DJ, Jung HY, Lee SH, Jung JK, Lee BC, Yun YP, *et al*. 2007 Increase of collagen synthesis by obovatol through stimulation of the TGF-beta signaling and inhibition of matrix metalloproteinase in UVB-irradiated human fibroblast. *J. Dermatol. Sci.* **46** 127–137

Dawes LJ, Angell H, Sleeman M, Reddan JR and Wormstone IM 2007a TGFbeta isoform dependent Smad2/3 kinetics in human lens epithelial cells: a Cellomics analysis. *Exp. Eye Res.* **84** 1009–1012

Dawes LJ, Elliott RM, Reddan JR, Wormstone YM and Wormstone IM 2007b Oligonucleotide microarray analysis of human lens epithelial cells: TGFbeta regulated gene expression. *Mol. Vis.* **13** 1181–1197

Dawes LJ, Sleeman MA, Anderson IK, Reddan JR and Wormstone IM 2009 TGFbeta/Smad4-dependent and -independent regulation of human lens epithelial cells. *Invest. Ophthalmol. Vis. Sci.* **50** 5318–5327

Eldred JA, Dawes LJ and Wormstone IM 2011 The lens as a model for fibrotic disease. *Philos. Trans. R. Soc. Lond. B. Biol. Sci.* **366** 1301–1319

Gotoh N, Perdue NR, Matsushima H, Sage EH, Yan Q and Clark JI 2007 An in vitro model of posterior capsular opacity: SPARC and TGF-beta2 minimize epithelial-to-mesenchymal transition in lens epithelium. *Invest. Ophthalmol. Vis. Sci.* **48** 4679–4687

Grocott T, Frost V, Maillard M, Johansen T, Wheeler GN, Dawes LJ, Wormstone IM and Chantry A 2007 The MH1 domain of Smad3 interacts with Pax6 and represses autoregulation of the Pax6 P1 promoter. *Nucleic Acids Res.* **35** 890–901

Hales AM, Chamberlain CG and McAvoy JW 1995 Cataract induction in lenses cultured with transforming growth factor-beta. *Invest. Ophthalmol. Vis. Sci.* **36** 1709–1713

Ji L, Liu T, Liu J, Chen Y and Wang Z 2007 Andrographolide inhibits human hepatoma-derived Hep3B cell growth through the activation of c-Jun N-terminal kinase. *Planta. Med.* **73** 1397–1401

Kayastha F, Madhu H, Vasavada A and Johar K 2014 Andrographolide reduces proliferation and migration of lens epithelial cells by modulating PI3K/Akt pathway. *Exp. Eye Res.* **128C** 23–26

Kerr CL, Huang J, Williams T and West-Mays JA 2012 Activation of the hedgehog signaling pathway in the developing lens stimulates ectopic FoxE3 expression and disruption in fiber cell differentiation. *Invest. Ophthalmol. Vis. Sci.* **53** 3316–3330

Kumar RA, Sridevi K, Kumar NV, Nanduri S and Rajagopal S 2004 Anticancer and immunostimulatory compounds from Andrographis paniculata. *J. Ethnopharmacol.* **92** 291–295

Lawler S, Feng XH, Chen RH, Maruoka EM, Turck CW, Griswold-Prenner I and Derynck R 1997 The type II transforming growth factor-beta receptor autophosphorylates not only on serine and threonine but also on tyrosine residues. *J. Biol. Chem.* **272** 14850–14859

Lee TY, Lee KC and Chang HH 2010a Modulation of the cannabinoid receptors by andrographolide attenuates hepatic apoptosis following bile duct ligation in rats with fibrosis. *Apoptosis.* **15** 904–914

Lee YC, Lin HH, Hsu CH, Wang CJ, Chiang TA and Chen JH 2010b Inhibitory effects of andrographolide on migration and invasion in human non-small cell lung cancer A549 cells via down-regulation of PI3K/Akt signaling pathway. *Eur. J. Pharmacol.* **632** 23–32

Li J, Huang W, Zhang H, Wang X and Zhou H 2007 Synthesis of andrographolide derivatives and their TNF-alpha and IL-6 expression inhibitory activities. *Bioorg. Med. Chem. Lett.* **17** 6891–6894

Liang FP, Lin CH, Kuo CD, Chao HP and Fu SL 2008 Suppression of v-Src transformation by andrographolide via degradation of the v-Src protein and attenuation of the Erk signaling pathway. *J. Biol. Chem.* **283** 5023–5033

Lin HY, Xu J, Ischenko I, Ornitz DM, Halegoua S and Hayman MJ 1998 Identification of the cytoplasmic regions of fibroblast growth factor (FGF) receptor 1 which play important roles in induction of neurite outgrowth in PC12 cells by FGF-1. *Mol. Cell Biol.* **18** 3762–3770

Liu CS, Wormstone IM, Duncan G, Marcantonio JM, Webb SF and Davies PD 1996 A study of human lens cell growth in vitro. A model for posterior capsule opacification. *Invest. Ophthalmol. Vis. Sci.* **37** 906–914

Mansfield KJ, Cerra A and Chamberlain CG 2004 FGF-2 counteracts loss of TGFbeta affected cells from rat lens explants: implications for PCO (after cataract). *Mol. Vis.* **10** 521–532

Nakerakanti S and Trojanowska M 2012 The Role of TGF-beta Receptors in Fibrosis. *Open Rheumatol. J.* **6** 156–162

Nathu Z, Dwivedi DJ, Reddan JR, Sheardown H, Margetts PJ and West-Mays JA 2009 Temporal changes in MMP mRNA

expression in the lens epithelium during anterior subcapsular cataract formation. *Exp. Eye Res.* **88** 323–330

Rabsilber TM and Auffarth GU 2006 [Pharmacological means to prevent secondary cataract]. *Klin. Monbl. Augenheilkd.* **223** 559-67

Radisky DC and LaBarge MA 2008 Epithelial-mesenchymal transition and the stem cell phenotype. *Cell Stem Cell.* **2** 511–512

Rajagopal S, Kumar RA, Deevi DS, Satyanarayana C and Rajagopalan R 2003 Andrographolide, a potential cancer therapeutic agent isolated from Andrographis paniculata. *J. Exp. Ther. Oncol.* **3** 147–158

Rana AC and Avadhoot Y 1991 Hepatoprotective effects of Andrographis paniculata against carbon tetrachloride-induced liver damage. *Arch. Pharm. Res.* **14** 93–95

Salh BS, Martens J, Hundal RS, Yoganathan N, Charest D, Mui A and Gomez-Munoz A 2000 PD98059 attenuates hydrogen peroxide-induced cell death through inhibition of Jun N-Terminal Kinase in HT29 cells. *Mol. Cell. Biol. Res. Commun.* **4** 158–165

Shen KK, Liu TY, Xu C, Ji LL and Wang ZT 2009 Andrographolide inhibits hepatoma cells growth and affects the expression of cell cycle related proteins. *Yao Xue Xue Bao.* **44** 973–979

Shen YC, Chen CF and Chiou WF 2000 Suppression of rat neutrophil reactive oxygen species production and adhesion by the diterpenoid lactone andrographolide. *Planta. Med.* **66** 314–317

Symonds JG, Lovicu FJ and Chamberlain CG 2006 Posterior capsule opacification-like changes in rat lens explants cultured with TGFbeta and FGF: effects of cell coverage and regional differences. *Exp. Eye Res.* **82** 693–699

Tsai HR, Yang LM, Tsai WJ and Chiou WF 2004 Andrographolide acts through inhibition of ERK1/2 and Akt phosphorylation to suppress chemotactic migration. *Eur. J. Pharmacol.* **498** 45–52

Walker JL, Wolff IM, Zhang L and Menko AS 2007 Activation of SRC kinases signals induction of posterior capsule opacification. *Invest. Ophthalmol. Vis. Sci.* **48** 2214–2223

Wang Q, Stump R, McAvoy JW and Lovicu FJ 2009 MAPK/ERK1/2 and PI3-kinase signalling pathways are required for vitreous-induced lens fibre cell differentiation. *Exp. Eye Res.* **88** 293–306

Wang W, Wang J, Dong SF, Liu CH, Italiani P, Sun SH, Xu J, Boraschi D, *et al*. 2010 Immunomodulatory activity of andrographolide on macrophage activation and specific antibody response. *Acta. Pharmacol. Sin.* **31** 191–201

WHO: Global data on visual impairments 2010. In: Available at: http://www.who.int/blindness/GLOBALDATAFINALforweb.pdf. Accessed June 30, 2010, Geneva, Switzerland, 2010.

Wormstone IM, Anderson IK, Eldred JA, Dawes LJ and Duncan G 2006 Short-term exposure to transforming growth factor beta induces long-term fibrotic responses. *Exp. Eye Res.* **83** 1238–1245

Wormstone IM, Del Rio-Tsonis K, McMahon G, Tamiya S, Davies PD, Marcantonio JM and Duncan G 2001 FGF: an autocrine regulator of human lens cell growth independent of added stimuli. *Invest. Ophthalmol. Vis. Sci.* **42** 1305–1311

Wormstone IM, Liu CS, Rakic JM, Marcantonio JM, Vrensen GF and Duncan G 1997 Human lens epithelial cell proliferation in a protein-free medium. *Invest. Ophthalmol. Vis. Sci.* **38** 396–404

Wormstone IM, Tamiya S, Anderson I and Duncan G 2002 TGF-beta2-induced matrix modification and cell transdifferentiation in the human lens capsular bag. *Invest. Ophthalmol. Vis. Sci.* **43** 2301–2308

MS received 22 April 2014; accepted 18 February 2015

Corresponding editor: Geeta Vemuganti